Taylor & Francis
Taylor & Francis Group

Environmental Hazards

ISSN: 1747-7891 (Print) 1878-0059 (Online) Journal homepage: www.tandfonline.com/journals/tenh20

Indicator-based risk assessments for urban hazard resilience: an application for flash floods

Despoina Skoulidou & Athanasia K. Kazantzi

To cite this article: Despoina Skoulidou & Athanasia K. Kazantzi (2025) Indicator-based risk assessments for urban hazard resilience: an application for flash floods, Environmental Hazards, 24:4, 339-364, DOI: 10.1080/17477891.2024.2396913

To link to this article: https://doi.org/10.1080/17477891.2024.2396913

© 2024 The Author(s). Published by Informa UK Limited, trading as Taylor & Francis Group

View supplementary material

Published online: 22 Sep 2024.

Submit your article to this journal

Article views: 1357

View related articles

View Crossmark data

Citing articles: 2 View citing articles

Full Terms & Conditions of access and use can be found at
https://www.tandfonline.com/action/journalInformation?journalCode=tenh20

ENVIRONMENTAL HAZARDS
2025, VOL. 24, NO. 4, 339–364
https://doi.org/10.1080/17477891.2024.2396913

Taylor & Francis
Taylor & Francis Group

OPEN ACCESS Check for updates

Indicator-based risk assessments for urban hazard resilience: an application for flash floods

Despoina Skoulidou [a,b] and Athanasia K. Kazantzi [c]

[a]Resilience Guard GmbH, Steinhausen, Switzerland; [b]CONSTRUCT-LESE, Faculty of Engineering, University of Porto, Porto, Portugal; [c]Department of Civil Engineering, School of Engineering, University of Birmingham, Birmingham, UK

ABSTRACT

Urban resilience to environmental hazards can be substantially improved if proactive planning is mainstreamed as a risk mitigation strategy. To enable such transition, a resource-efficient and transparent framework is urgently needed for undertaking vulnerability and risk assessments, to consequently inform risk-aware proactive planning on spatially variable assets with very diverse characteristics. This study proposes an indicator-based risk-assessment framework, for efficiently treating the spatially distributed diverse physical and social components comprising a city network. The proposed framework decomposes the risk to its three main dimensions, i.e. hazard, exposure and vulnerability; with the latter accounting for both the susceptibility of the city network to the considered hazard and its capacity to cope. The inclusion of the capacity to cope as a distinct element, that accounts for both city and building-block level preparatory actions, is a unique feature, much sought in Decision Support Systems, that allows to directly quantify their effectiveness towards risk mitigation. The outcome of spatially variable risk estimates, could be exploited by urban planners and city authorities for undertaking risk-aware urban design, development and resilience enhancement decisions. The framework is demonstrated herein for the case of flash floods but could be tailored to accommodate other types of environmental hazards.

ARTICLE HISTORY
Received 26 April 2024
Accepted 21 August 2024

KEYWORDS
Risk; vulnerability; coping capacity; proactive adaptation; decision support system; indicators

1. Introduction

Vulnerability and risk assessment methodologies for environmental perils have become a matter of uppermost importance for pre-disaster management, with pertinent organisations and working groups (e.g. see FEMA, 2019; IPCC, 2022a) investing a great deal of effort and resources towards their development, verification and mainstreaming. Earthquakes, floods and air quality degradation are just a few indicative perils that could

CONTACT Athanasia K. Kazantzi a.kazantzi@bham.ac.uk Department of Civil Engineering, School of Engineering, University of Birmingham, Edgbaston, B15 2TT, Birmingham, UK

Supplemental data for this article can be accessed online at https://doi.org/10.1080/17477891.2024.2396913.

© 2024 The Author(s). Published by Informa UK Limited, trading as Taylor & Francis Group
This is an Open Access article distributed under the terms of the Creative Commons Attribution License (http://creativecommons.org/licenses/by/4.0/), which permits unrestricted use, distribution, and reproduction in any medium, provided the original work is properly cited. The terms on which this article has been published allow the posting of the Accepted Manuscript in a repository by the author(s) or with their consent.

adversely impact cities, inducing negative consequences to their inhabitants as well as to their built and natural environment. Such adverse impacts may involve disruptions to business and critical services, structural and non-structural damages, injuries, health-related issues or even fatalities as well as monetary losses (e.g. see Loli et al., 2022; Taramelli et al., 2022; Yuan, 2008). Recent evidence on the aggravation of several environmental perils due to climate change along with the ever-increasing urbanisation of the already densely populated contemporary cities, render the importance of risk-informed proactive management even more emerging (UNISDR, 2015).

There are currently available different methodologies for assessing the risk associated with a spectrum of environmental hazards. Depending on the scale of the assessment and the data available, quantitative risk assessments are based on vulnerability or fragility curves, while semi-quantitative ones are mostly based on indicators that offer comparative risk scores instead of explicit probabilities or other measurable consequences (Simmons et al., 2017). Among the most informative, but also most demanding in terms of the needed resources, are the quantitative methodologies (e.g. see Gentile et al., 2022; Mitoulis et al., 2023). Such methodologies provide a relatively good understanding of the underlying vulnerability mechanisms, dependencies and risk sources and could be efficiently exploited in the design of appropriate adaptation measures (Fuchs et al., 2012). On the other hand, semi-quantitative methodologies, that are founded upon vulnerability and risk indicators and indices (e.g. Balica et al., 2012; Leal et al., 2021; Nelson & Ahmadpoor, 2023; Rana & Routray, 2018a), aim to identify and quantify the risk based on the collection and combination of certain indicators (Fuchs et al., 2012). Despite being popular for evaluating the social vulnerability component for many years now (e.g. see Schmidtlein et al., 2008), indicator-based approaches attracted less attention in studies that were focused on assessing the physical vulnerability component (e.g. see Silva & Pereira, 2014). The main disadvantage of such indicator-based vulnerability assessment approaches, is that they are intensity-agnostic (Papathoma-Köhle, 2016). Yet, this latter property fits well the needs of an urban-scale assessment. Both of the abovementioned methodologies may be considered being quantitative, while qualitative alternatives are also possible, by however trading accuracy for efficiency. This could be done for instance via estimating vulnerability and risk by means of the so-called vulnerability and risk matrices (e.g. Kang & Kim, 2016; Papathoma-Köhle et al., 2017).

For urban-scale risk assessment applications, the availability of the underlying data along with practicality-related aspects, favour the use of indicator-based methods like those that are founded upon indicator metrics (e.g. Bruneau et al., 2003; Cutter et al., 2010; Morrison et al., 2022). In a number of such earlier attempts, the main effort has been put towards assessing the capacities via a set of indicators that could have an impact on the disaster resilience of the communities. Yet, the utilised capacity indicators are mostly assessed on a global scale and hence could not inform local adaptation measures. Moreover, the effect of such capacity metrics was assumed to be uniform across the investigated network. This is a capability gap that needs to be addressed to make a risk assessment framework suitable for use in practical applications aiming to: (a) identify local or global interventions that could mitigate the disaster risk and (b) prioritise them on the basis of risk-based knowledge (Cutter & Derakhshan, 2020) that is used for assessing their efficiency. This research study offers a practical semi-quantitative, urban-scale risk assessment framework that utilises indicator-based approaches to

identify the most stressed parts of a city network, should the latter be affected by an environmental hazard. The proposed framework could be exploited, in a first-order risk-aware Decision Support System (DSS), that aims to assist urban-planners and decision-makers prioritising and consequently directing the available resources in the most efficient proactive city and building-block level adaptation measures (Kontopoulos et al., 2023).

2. Definition of risk and its components

The risk concept has been extensively used for several decades now. However, the definition of risk and its components has puzzled scientists, researchers and practitioners (Wolf, 2012), since the relevant terms are often used interchangeably across literature, leading to lack of consistency and ultimately to confusion (Fuchs et al., 2024; Liverman, 1990; Nguyen et al., 2016; Sun & Liu, 2024; Waseem & Rana, 2023). This lack of consistency in the risk terminology, essentially reflects the evolutions occurring in the disaster risk field, and it is outlined in detail by Kelman (2018). In the present study, in accordance with IPCC (2019, 2022a), that essentially adapted the risk concept as this was defined and evolved over the years in several different research studies and various sources (e.g. IPCC, 2014; ISO, 2021; UNDRR, 2016; Wisner et al., 2004), risk comprises a function of hazard (*H*), exposure (*E*) and vulnerability (*V*) [see Eq.(1)]. In this function, hazard characterises the intensity and the likelihood/frequency of the peril, exposure accounts for the assets (e.g. people, buildings) that are exposed to the peril and are likely to sustain/experience some kind of loss/damage, whereas vulnerability refers to the predisposition of such assets to be adversely affected when exposed to the investigated peril, and is evaluated on the basis of two sub-components, these being (i) the susceptibility (*S*) to harm/damage and (ii) the lack of capacity to cope (*COP*) [see Equation (2)] (Adger, 2006; IPCC, 2022b; IPCC, 2023). The capacity to cope accounts for the defence mechanisms, the problem-solving techniques as well as methods for handling a particular stress (Murphy & Moriarty, 1976; Wisner et al., 2004). The risk as defined herein, is essentially a proxy for quantifying the consequences of environmental hazards on the exposed vulnerable assets (IPCC, 2014) across the investigated region, to allow identification of the risk hot-spots (Hawchar et al., 2020).

$$\text{Risk} = f(H, E, V) \tag{1}$$

$$V = f(S, COP) \tag{2}$$

Moreover, in order to account for the risk multidimensionality, two distinct dimensions of the exposure and the susceptibility components, the social (*SO*) and the physical (*PH*), are identified and consequently are treated separately. Additional risk dimensions that are often found in the existing literature, especially for the susceptibility subcomponent, such as the economic and environmental (e.g. Abdrabo et al., 2023; Cutter et al., 2003; Fekete et al., 2010; Rana & Routray, 2018b), are accounted for in the present study only in an implicit manner.

By definition, the vulnerability component is among the hardest to define in an urban-scale risk assessment, since the physical and social elements formulating the urban environment are (a) numerous, (b) highly spatially distributed and (c) not consistently

vulnerable across the different perils that are likely to affect them (e.g. Ciurean et al., 2013). Furthermore, as stated by Birkmann (2007), the definition of the vulnerability component could be different not only due to the different nature of the considered perils but also due to the distinct characteristics of each community. Hence, certain adjustments are likely to be needed on account of the function that is served by the assessment as well as the physical, social and economic particularities in the region of interest.

3. Proposed urban-scale indicator-based framework

3.1. Selection of indicators

The selection of indicators for defining the three risk components, is the first step that needs to be taken in the proposed framework. Although there exist no specific guidelines for performing this action, some common rules apply. Herein, the selection process accounts for the existing literature, field knowledge and/or expert judgement, considering the peril of interest, the distinct characteristics of the examined area as well as the anticipated outcome. The process of selecting an appropriate list of indicators that are significantly correlated with the susceptibility or intrinsic vulnerability (Leal et al., 2021) of the physical and the social assets exposed to a considered peril, is an important aspect in the development of the indicator-based risk assessment framework. Particular attention should be paid in excluding indicators that are highly correlated, to avoid accounting twice for the same property. The vulnerability, exposure and hazard indicators that will formulate the final list, should be selected, among others, to be measurable, based on available data, sensitive and specific (Birkmann, 2013).

3.2. Scoring of indicators

Given the diverse nature of the selected indicators, there exist several different scales for measuring them. However, it is essential that all indicators are expressed in a common scale to render their aggregation meaningful, in the sense that their actual value should not affect unequally the outcome. In the proposed framework, all indicators were assigned scores that vary between 0 and 1. In the case of indicators with ordered descriptive scales (i.e. scales with a finite number of ranges/categories) each range was assigned a score in the aforementioned range. In case of indicators with continuous scales, their scores were computed via normalising the indicators, utilising the *min–max* normalisation formula

$$x_{Norm,\,i} = \frac{x_i - x_{min}}{x_{max} - x_{min}} \tag{3}$$

where x_i is the unnormalised data point of the ith indicator, x_{min} is the minimum value of the ith indicator and x_{max} is the maximum value of the ith indicator. The maximum (*max*) and minimum (*min*) values do not always reflect the boundaries of the considered dataset, since in many cases the latter reflects just a fraction of the values that are likely to be encountered. Hence, the *min* and *max* values of an indicator should be based either on historical data or on expert opinion.

By contrast, qualitative indicators may be binary (e.g. yes/no) and consequently could, by definition, be paired to a score equal to either 1 or 0. An example of a binary indicator is the existence of an extreme temperature early warning system that could improve the

coping capacity of the city to the said peril. In some other cases, qualitative indicators could be defined by considering a spectrum of options and assign a score to each one of them that ranges between 0 and 1. For instance, a building could be assigned, on account of the number of its storeys, to three different categories: (a) one-storey, (b) two-storey and (c) more than two-storey and consequently each of these options receives a score that reflects the damage propensity of this building to flash flood events due to its height (e.g. equal to 1, 0.5 and 0.33, respectively as per Leal et al., 2021).

3.3. Urban indicator-based vulnerability assessment

The proposed indicator-based urban-scale vulnerability assessment disaggregates the urban vulnerability component into three main elements/sub-components and consequently to three different kinds of vulnerability indicators, these being: (a) the 'physical susceptibility', that quantifies how prone to peril-induced damages is the urban built environment, (b) the 'social susceptibility', that assesses the harm potential of the people exposed to the considered peril and (c) the 'capacity to cope' element, that accounts for those characteristics/properties/measures that could contribute in mitigating the physical and social susceptibility.

Following the identification of the appropriate vulnerability indicators, these are assigned scores and are consequently combined utilising an appropriate aggregation method to deliver the associated susceptibility/capacity to cope sub-components. The weighted arithmetic average was adopted for combining/aggregating the susceptibility and coping capacity indicators to eventually form the three vulnerability sub-components according to the following expressions:

Physical susceptibility:

$$S_{PH} = w_{S_{PH1}} \cdot S_{PH1} + w_{S_{PH2}} \cdot S_{PH2} + \ldots + w_{S_{PHi}} \cdot S_{PHi} \tag{4}$$

Social susceptibility:

$$S_{SO} = w_{S_{SO1}} \cdot S_{SO1} + w_{S_{SO2}} \cdot S_{SO2} + \ldots + w_{S_{SOj}} \cdot S_{SOj} \tag{5}$$

Coping capacity:

$$COP = w_{COP_1} \cdot COP_1 + w_{COP_2} \cdot COP_2 + \ldots + w_{COP_k} \cdot COP_k \tag{6}$$

where, $w_{S_{PHi}}$, $w_{S_{SOj}}$, w_{COP_k} are the weights attributed to the *i*th indicator expressing physical susceptibility, the *j*th indicator expressing social susceptibility and the *k*th indicator expressing the capacity to cope, respectively, and S_{PHi}, S_{SOj} and COP_k are the physical susceptibility, social susceptibility and coping capacity indicator scores, respectively. The weights assigned to the indicators of each vulnerability dimension need to satisfy the following conditions:

$$\sum w_{S_{PHi}} = 1, \ \sum w_{S_{SOj}} = 1, \ \sum w_{COP_k} \leq 1 \tag{7}$$

In the presented framework, the vulnerability component is defined via combining the vulnerability sub-components, that is, the total susceptibility (physical and social) and the lack of coping capacity (1-*COP*) according to the following equation:

$$V = (W_{S_{PH}} \cdot S_{PH} + W_{S_{SO}} \cdot S_{SO}) \cdot (1 - COP) \tag{8}$$

where, $W_{S_{PH}}$ and $W_{S_{SO}}$ are the weights attributed to the physical and social susceptibility dimensions, respectively, which should also add to 1.0.

The inclusion of the capacity to cope as a separate urban vulnerability component provides direct and quantifiable answers to the pertinent authorities as to what can be modified, newly implemented or done differently at a local or global scale so as to improve the performance of the city network to the considered peril. The proposed vulnerability discretisation, that involves the identification of the main city or building block-scale strengths and weaknesses, fully serves the needs of a risk-aware DSS. It is also highlighted that the sum of w_{COP_k} could be either equal to or – for most practical applications – lower than 1 (if implementing all available coping capacity measures is not sufficient to fully eliminate the existing vulnerabilities), depending on the available measures to mitigate vulnerability as well as their efficiency.

An additional advantage of the proposed combination rule for estimating the vulnerability component, as reflected in Equation (8), lies in the addition of the two susceptibility dimensions, that is, physical and social, that allows for the consideration of each dimension independently and regardless of the existence of the other. By contrast, the aggregation of the total susceptibility with the lack of coping capacity is performed by means of multiplication. The multiplication of the two sub-components allows for the vulnerability score to take its maximum value, i.e. equal to the total susceptibility score, in case of complete absence of coping capacity. Furthermore, depending on the weights assigned to the COP indicators, the implementation of one or more COPs can lead to a faster or slower reduction of the vulnerability score.

3.4. Urban indicator-based exposure assessment

The exposure component of the risk, accounts for the assets that are present in the area of interest and are likely to be affected and/or experience any kind of damage/loss during the occurrence of the hazard. Following a procedure similar to the one adopted for the vulnerability component, the exposure component in this study is discretised into indicators that account for the physical and the social exposure, and thus forming the following two exposure sub-components:

Physical exposure:

$$E_{PH} = w_{E_{PH1}} \cdot E_{PH1} + w_{E_{PH2}} \cdot E_{PH2} + \ldots + w_{E_{PHq}} \cdot E_{PHq} \tag{9}$$

Social exposure:

$$E_{SO} = w_{E_{SO1}} \cdot E_{SO1} + w_{E_{SO2}} \cdot E_{SO2} + \ldots + w_{E_{SOr}} \cdot E_{SOr} \tag{10}$$

where, $w_{E_{PHq}}$, $w_{E_{SOr}}$ are the weights attributed to the qth and rth indicators expressing physical exposure and social exposure, respectively, and E_{PHq} and E_{SOr} are the physical exposure and social exposure indicator scores, respectively. The weights assigned to the indicators of each exposure sub-component need to satisfy the following conditions:

$$\sum w_{E_{PHq}} = 1 \text{ and } \sum w_{E_{SOr}} = 1 \tag{11}$$

Physical exposure indicators include metrics/measures that account for the building stock in the urban area of interest, for example, number of buildings or built area

density, while social exposure indicators account for the people living, working and/or commuting in the area, for example, population density.

The aggregation of the exposure sub-components into the exposure component is performed according to the following combination rule:

$$E = W_{E_{PH}} \cdot E_{PH} + W_{E_{SO}} \cdot E_{SO} \tag{12}$$

where, $W_{E_{PH}}$ and $W_{E_{SO}}$ are the weights attributed to the physical and social exposure dimension, respectively adding to 1.0.

3.5. Urban indicator-based hazard assessment

The hazard assessment involves the estimation of the probability that a hazardous event of a particular intensity will occur within a specific timeframe at a particular location. In the proposed indicator-based framework, the score associated with the hazard index H is evaluated as per Equation (13) on account of a considered hazard scenario, as the product of (a) the score assigned to the hazard intensity indicator, *Intensity* (considering low up to extremely high intensities, with higher scores assigned to higher intensities) that accounts for the magnitude of the hazard event (e.g. inundation depth) associated with the said scenario and (b) the score assigned to the likelihood indicator, *Likelihood* (ranging from frequent to very rare, with higher scores assigned to more frequent events) that depicts the mean return period of the considered hazard scenario. Hence, on account of the above the hazard component score for a certain hazard scenario may be evaluated as:

$$H = Intensity \cdot Likelihood \tag{13}$$

The *Likelihood* may be set to 1.0, to either investigate '*what-if*' scenarios or if the performance of the city network is evaluated considering past events (to for instance calibrate the framework or different risk mitigation measures). In such cases, the likelihood of the event is irrelevant, since the event is essentially considered to be deterministic, rather than uncertain.

3.6. Urban indicator-based risk assessment

In the proposed framework, the risk score is ultimately calculated via aggregating the previously determined exposure (E), vulnerability (V) and hazard (H) scores as follows:

$$R = \sqrt[3]{E \cdot V \cdot H} \tag{14}$$

The geometric mean is adopted herein for the aggregation of the risk component scores, instead of the more commonly used arithmetic mean, since it (i) satisfies the condition of returning zero risk score estimates for a certain location in case of complete absence of any one of the risk elements, i.e. exposure, vulnerability or hazard (Marin-Ferrer et al., 2017), and (ii) provides risk score estimates that remain within the range of the risk components.

3.7. Weighting methods for the evaluation of indices

The process of aggregating the indicators to eventually compute a composite index, for example, the physical susceptibility, includes also the definition of their weights.

According to Papathoma-Köhle et al. (2019) this process is the most sensitive step among those that need to be taken for evaluating the required indices. In the literature, there are currently available several different approaches for estimating the indicator weights, such as methods that are based on statistical analysis, for example, the principal component analysis (PCA) and the factor analysis, methods that are based on expert judgment, for example, the analytical hierarchy process (AHP) and the budget allocation process, as well as the equal weighting approach. However, no established generic approach currently exists on how to select the most appropriate weighting method.

PCA is a method developed to reduce the dimensionality of a dataset, while preserving the required variability, but it could also be applied for weight derivation, given that the examined dataset has only one principal component. The PCA method is a statistically based, objective option for weight selection that depends on the considered dataset. However, the weights determined according to the PCA are based on correlations of the sub-indicators which do not necessarily reflect the underlying relationships between the sub-indicators and the phenomena being measured (Saisana & Tarantola, 2002). Furthermore, the method may become ambiguous if some indicators are defined in a binary manner (Collins et al., 2002). On the other hand, AHP proposed by Saaty (1990), offers a methodological framework for assessing the relevant importance in a set of indicators, based on how the importance of each one of them is judged against the importance of the others by a group of experts in the pertinent field (Kumar et al., 2021). AHP constitutes a predominantly subjective weighting approach that requires expert judgement.

The most commonly used weighting method, is the equal weighting (Papathoma-Köhle et al., 2019). The equal weighting approach is founded on the assumption that all indicators contribute equally to the relevant composite index. The reasons for being the prevailing weighting choice can be attributed to its simplicity, claimed objectivity and possible lack or inadequacy of theoretical and/or empirical knowledge that would justify the adoption of more complex weighting schemes (Greco et al., 2019; Mikulic et al., 2015). Moreover, as stated by Esty et al. (2005), data-dependent weighting methods (e.g. PCA) do not always reflect the priorities of the decision-makers or other constraints (e.g. budget).

In the proposed framework, the equal weight approach was used for all indicators, except for the coping capacity ones in which case unequal weighting was adopted based on expert judgement. An overall workflow of the framework is presented in Figure A of the supplementary file.

4. Case study application for the city of Milan affected by flash flooding

4.1. Case study area

To showcase the proposed risk assessment framework, an example application is presented for the case of flash flood in the city of Milan, that is the second most populated Italian city [see Figure 1(a)]. Flash floods are deemed to be sudden local flood incidents that are characterised by high water volumes and short duration following a heavy precipitation event. In the past, Milan was affected by several flash flood incidents and hence in the '70s a number of flood protection measures were implemented in the city (Ravazzani et al., 2016). One such measure is the construction of a bypass channel of the Seveso

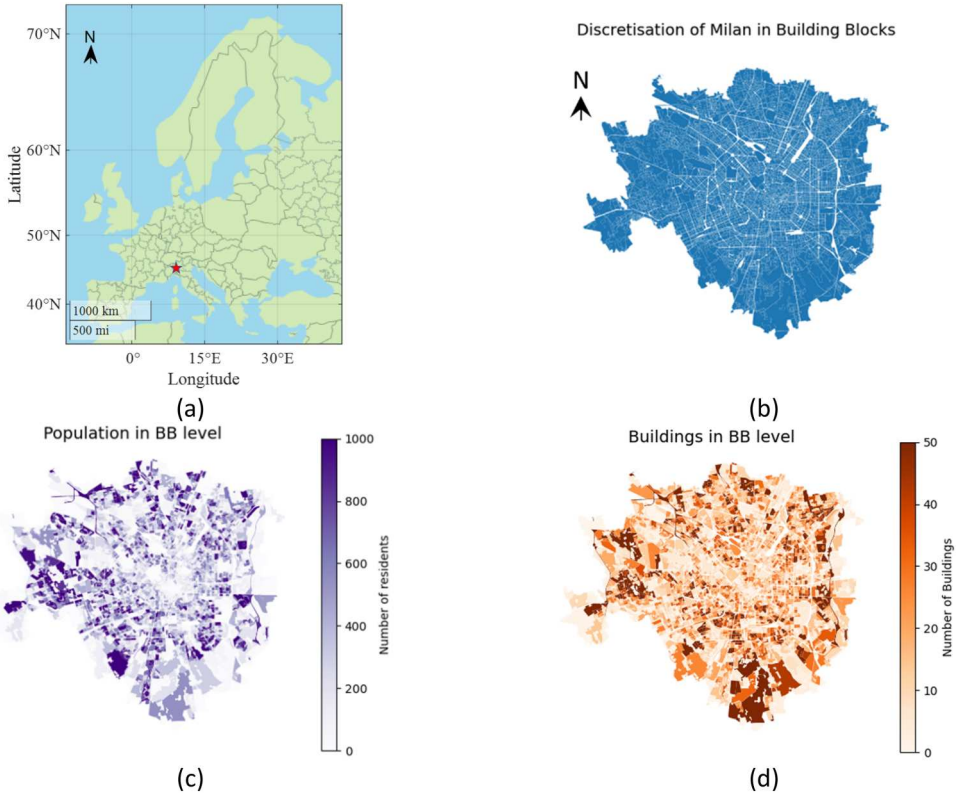

Figure 1. (a) Location of the city of Milan in Europe, (b) discretisation of Milan in BBs, (c) number of residents per BB level and (d) number of buildings per BB level.

River, in which the excess discharge is directed (Becciu et al., 2018). However, the recent occurrence of flash floods showcased that the capacity of such protection measures is often exceeded and hence the city remains prone to the flood peril.

The spatial resolution to which the risk components and consequently risk scores are offered is highly dependent on the resolution of the available data (Morrison et al., 2022). In the present case study, the Building Block (BB) level spatial resolution is adopted and hence all indicator and risk component scores are derived per BB. Figure 1(b) shows the discretisation of Milan city in BBs, while Figure 1(c) and 1(d) illustrate the spatial distribution of the population (number of residents) and the number of buildings in each BB, respectively.

4.2. Selection and scoring of the vulnerability indicators for the flash flood peril

The build-up of the vulnerability component is demonstrated in this section for the case of flash flood. Table 1 summarises the vulnerability indicators that are proposed for depicting the three dimensions which are accounted for in this component, i.e. the physical (PH), the social (SO) and the capacity to cope (COP). The list of indicators presented in Table 1 is not exhaustive, although is deemed to be characteristic for the considered hazard in the region of interest (and more likely appropriate to other cities that have similar physical and social characteristics). Table A of the Supplementary file provides

Table 1. Vulnerability, exposure and hazard indicators selected for the flash flood peril in Milan.

Category	Name	Indicator	Weight (w)	References
Physical susceptibility	PH1	Construction material (CM)	0.25	Leal et al. (2021), Taramelli et al. (2022), Muller et al. (2011)
	PH2	Conservation status (CS)	0.25	Kappes et al. (2012), Leal et al. (2021), Taramelli et al. (2022)
	PH3	Number of storeys (NS)	0.25	Kappes et al. (2012), Leal et al. (2021), Stephenson and D'Ayala (2014)
	PH4	Age of construction (AC)	0.25	Leal et al. (2021), Taramelli et al. (2022), Zhen et al. (2022)
Social susceptibility	SO1	Percentage of older adults 65 and over (Eld65)	0.25	Karagiorgos et al. (2016), Chang et al. (2021).
	SO2	Percentage of children under 15 (Chi15)	0.25	Cutter et al. (2003), Chang et al. (2021), Moreira et al. (2021), Karagiorgos et al. (2016)
	SO3	Unemployment rate (UR)	0.25	Karagiorgos et al. (2016), Krellenberg and Welz (2017)
	SO4	Education level (EL)	0.25	Karagiorgos et al. (2016), Cutter et al. (2003).
Coping capacity	COP1	Early warning system (EWS)	0.10	Pathak et al. (2020)
	COP2	Maintenance of drainage system (DSM)	0.20	
	COP3	Past experience with major floods (PEF)	0.05	Pathak et al. (2020), Muller et al. (2011), Hidayah et al. (2021), Karagiorgos et al. (2016), Vitale and Meijerink (2021).
	COP4	Flood protection infrastructure (FPI)	0.40	Bigi et al. (2021).
	COP5	Percentage of greenery within 100 m (PG)	0.20	Kim et al. (2016), Muller et al. (2011), Niehoff et al., 2002.
	COP6	Awareness on the flood hazard (AFH)	0.05	Karagiorgos et al. (2016), Pathak et al. (2020), Stephens et al. (2024)
Hazard	Intensity1	Flood inundation depth (FID)		Zischg et al. (2021), Leal et al. (2021), Maranzoni et al. (2023)
Exposure	EX_PH1	Building density (BD)		Thouret et al. (2014)
	EX_SO1	Population density (PD)		Bigi et al. (2021)
		Critical infrastructure		

information regarding the susceptibility and capacity to cope scores of the selected indicators along with a brief description. The scores were mainly founded on evidences from existing literature or on expert judgement.

4.3. Physical susceptibility for the flash flood peril

The data required for calculating the four indicators scores that were selected to depict the physical susceptibility were obtained from the Italian National Institute of Statistics (i.e. Census data). Figure 2(a)–(d) illustrates the spatial distribution of the construction material (CM, PH1), the conservation status (CS, PH2), the number of storeys (NS, PH3) and the age of construction (AC, PH4) scores, respectively.

4.4. Social susceptibility for the flash flood peril

The data required for the calculation of all four selected social susceptibility indicators were obtained from the Italian National Institute of Statistics. The spatial variability of the social susceptibility scores related to the percentage of elderly (eld65, SO1), the percentage of children (chi15, SO2), the unemployment rate (UR, SO3) and the educational level (EL, SO4) across the city of Milan are presented in Figure 3(a)–(d), respectively.

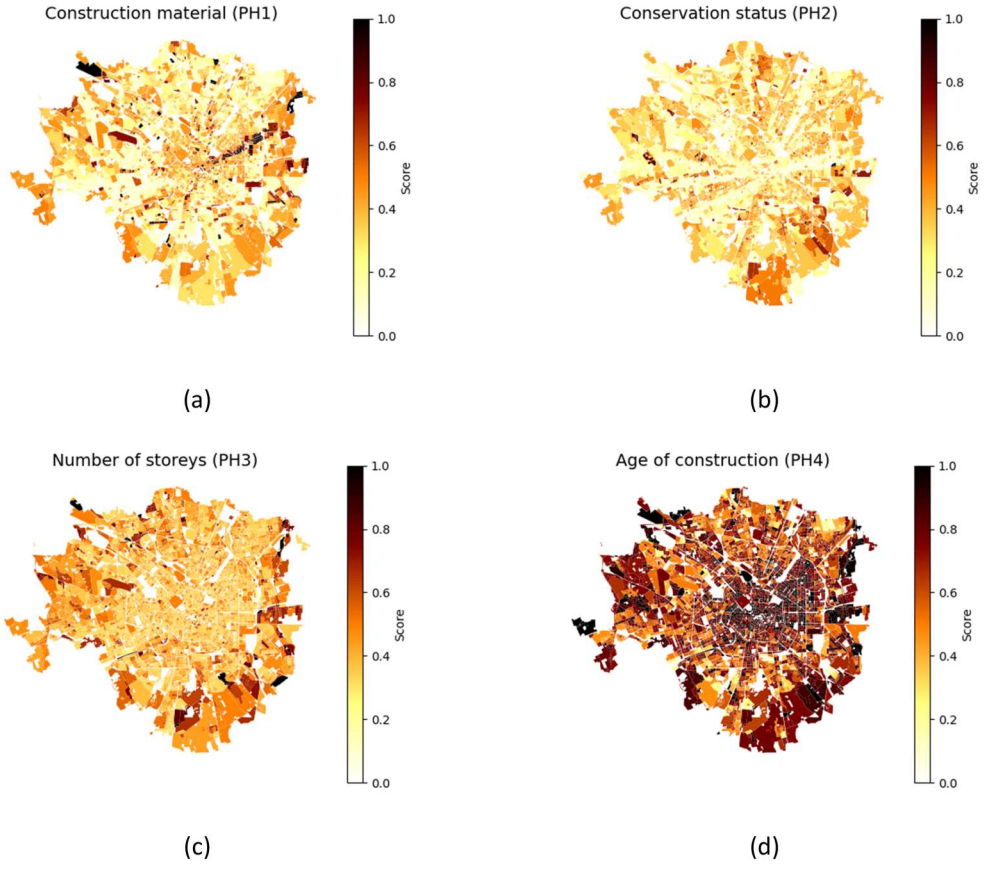

Figure 2. Spatial variability of the physical susceptibility scores related to (a) the construction material (PH1), (b) the conservation status (PH2), (c) the number of storeys (PH3), and (d) the age of construction (PH4).

4.5. Coping capacity for the flash flood peril

The six indicators that were selected to address the capacity to cope in flash floods, are presented in Table 1. The majority of these indicators are defined in areas that exceed the BB level, which was selected as the working resolution level in the considered case study. This essentially implies that those coping capacity measures affect the ability of the entire city or a large portion of it to cope with the peril, and hence, in such cases, the same coping capacity scores are assigned to the BBs of the said areas.

Measuring the exact effect of the various actions/interventions on the risk across a spectrum of perils is a complex process which becomes even more challenging to address within the context of an indicator-based assessment. Nevertheless, the scope herein is mainly to develop a framework upon which a risk-aware DSS could be founded rather than to offer exact risk score estimates. Hence, what it is mostly of interest is the relevant impact of one preventative action (local or global) against another one on the risk estimates. For certain mitigation measures, the exact impact, once the actions are being prioritised, may be determined through detailed modelling.

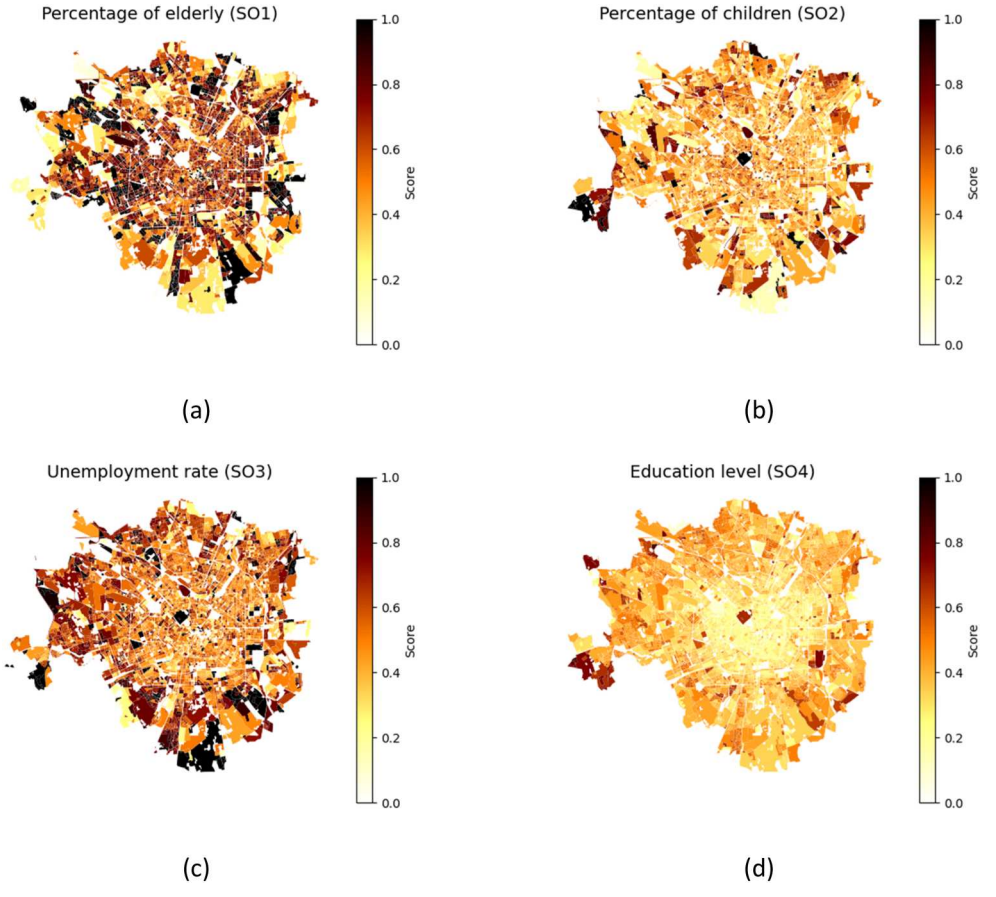

Figure 3. Spatial variability of the social susceptibility indicator scores related to (a) the percentage of elderly (SO1), (b) the percentage of children (SO2), (c) the unemployment rate of the population (SO3), and (d) the education level (SO4).

Information regarding the actual COPs already implemented in the city of Milan was provided by the Urban Resilience Department of the Municipality of Milan. As such, the 'yes' option (see Table A of supplementary file) implies the existence of an EWS and hence a score equal to 1.0 is assigned to all BBs for COP1. The 'occasionally maintained' option applies to the DSM for the city of Milan and hence a score equal to 0.5 was assigned to COP2 for undertaking the baseline assessment (i.e. the 'as is' performance of the city network). Information provided by the by the Urban Resilience Department of the Municipality of Milan indicated that the city suffers from major flood events almost every year. Hence, a score equal to 1.0 was attributed to COP3. Various flood protection infrastructure measures can be found in the city of Milan, yet their adequacy is questionable given the several recent severe flash flood incidents (Ravazzani et al., 2016) and thus a score equal to 0.0 was initially assigned to COP4 for the baseline assessment. Awareness on the flood hazard is assumed for the residents of Milan and hence, a score equal to 1.0 is assigned to COP6 and for all BBs. Contrary to the above, the COP associated with the percentage of greenery was calculated based on land cover geoinformation. The derived coping capacity scores related to the percentage of greenery in a 100

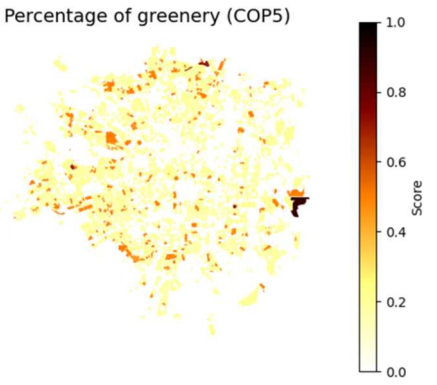

Figure 4. Spatial variability of the coping capacity indicator score related to the percentage of greenery in 100 m radius area (COP5).

m radius area (COP5) from the geometric centre of each BB are shown in Figure 4 for the city of Milan. Consequently, if the greenery in any BB is increased within a risk mitigation scenario, then the total percentage of greenery (existing and additional) should be considered for the determination of the updated COP5 scores.

4.6. Aggregation of the vulnerability indicators for the flash flood peril

The four selected physical susceptibility indicators, i.e. CM, CS, NS and AC (see Table 1), are aggregated into the physical susceptibility sub-component (S_{PH}) based on the weighted average [see Equation (4)], where the weights of the indicators (w_{CM}, w_{CS}, w_{NS} and w_{AC}) are assumed to be equal, hence all being set to 0.25. Similarly, the equal weight approach is used for aggregating the selected four social susceptibility indicators, i.e. Eld65, Chi15, UR and EL (see Table 1), into the social susceptibility sub-component (S_{SO}) [see Equation (5)], with w_{Eld}, w_{Chi}, w_{UR} and w_{EL} set equal to 0.25. The selected six coping capacity indicators, that is, EWS, DSM, PEF, FPI, PG and AFH (see Table 1), are aggregated into the coping capacity sub-component (COP) [see Equation (6)] following an unequal weight approach, with w_{EWS}, w_{DSM}, w_{PEF}, w_{FPI}, w_{PG} and w_{AFH} assigned values equal to 0.10, 0.20, 0.05, 0.40, 0.20 and 0.05, respectively based on expert judgement (note that the weights of the considered COPs add to 1 for the case at hand, but this is not a prerequisite of the proposed framework). The highest weight, i.e. 0.40, is assigned to COP4 (FPI). This is the COP indicator associated with the construction of new code-conforming flood protection infrastructure (or an appropriate enhancement of the capacity of the existing one), as this counter measure is anticipated to have the highest positive impact on the flood resilience of the community and the built environment. The percentage of greenery (PG, COP5) and the maintenance of the drainage system (DSM, COP2) COP indicators are assigned weights equal to 0.20 each, followed by the early warning system (EWS, COP1) that was assigned a weight equal to 0.10. The lowest weights are assigned to the COPs related to past experience with major floods (PEF, COP3) and the population awareness of the flash flooding hazard (AFH, COP6), i.e. set equal to 0.05. Figure 5(a)–(c) shows the spatial distribution of the scores for the three vulnerability sub-components derived for the case-study city of Milan. It should be noted that for a more accurate

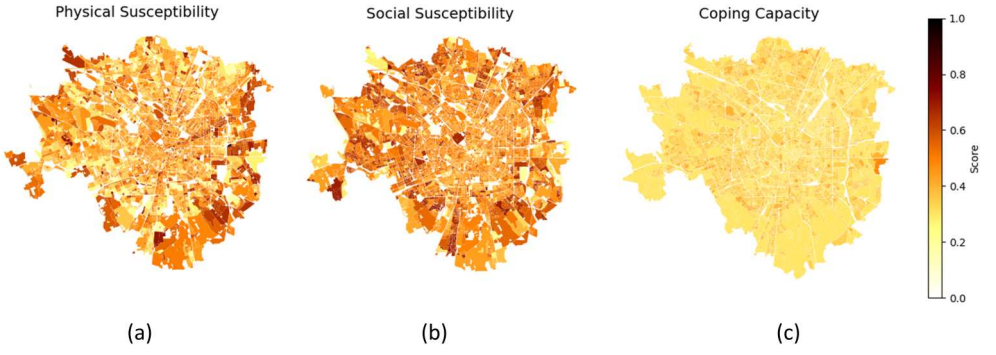

Figure 5. Spatial distribution of (a) the Physical susceptibility, (b) Social susceptibility and (c) the Coping capacity scores for the city of Milan.

definition of the weights extensive verification of the vulnerability estimates with historical data is required.

Assuming an equal contribution for the two susceptibility sub-components, that is, $W_{S_{PH}} = W_{S_{SO}} = 0.5$, the total susceptibility score per BB is determined and presented in Figure 6(a), along with the lack of coping capacity score (evaluated as 1-*COP*), presented in Figure 6(b). Finally, the aggregation of the three vulnerability sub-components into the vulnerability component (*V*), which represents the BB vulnerability score, is performed according to Equation (8). Figure 6(c) shows the spatial distribution of the vulnerability scores in all BBs of the Milan city. The relatively low vulnerability scores (<0.5) determined for most parts of the city are attributed to both the moderate inherent total susceptibility (average susceptibility score ~0.6) as well as to the existing COP measures already implemented in the city (average lack of coping capacity score ~0.7).

4.7. Selection and scoring of the exposure indicators for the flash flood peril

The evaluation of the exposure component of the risk follows a similar approach to that adopted in the case of the vulnerability components, as already discussed in Section 3.4.

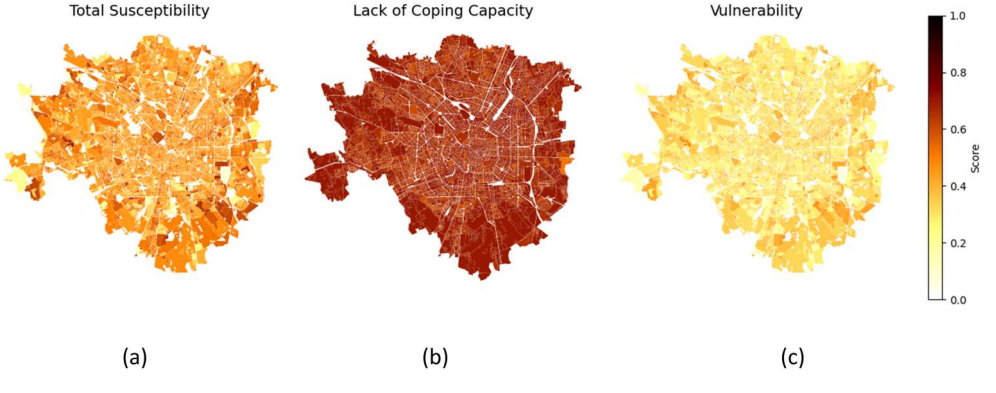

Figure 6. Spatial distribution of (a) the total susceptibility, (b) the lack of coping capacity, and (c) the vulnerability scores for the city of Milan.

Hence, social and physical exposure sub-components are considered separately and are consequently aggregated for defining the overall exposure component score.

Figure 7(a) illustrates the BBs in which critical infrastructure exists in the city of Milan, whereas Figure 7(b) and (c) present the spatial variability of the physical and social exposure scores accounting for the critical infrastructure. Higher physical exposure scores are observed close to the centre of Milan, essentially reflecting the denser urban fabric of the city centre compared to the surrounding areas, whereas both high and low social exposure scores are scattered across the city without showing any constant trends. All BBs with critical infrastructure were assigned the maximum score, i.e. 1, both in their physical and social exposure elements and hence appear in the pertinent figures in black colour.

4.7.1. Aggregation of the exposure components

Following the identification of the exposure indicators, the collection of data and their scoring, the aggregation of E_{PH} and E_{SO} is performed based on the weighted average [Equation (12)] and an equal weight assumption, i.e. $W_{E_{PH}} = W_{E_{SO}} = 0.5$. The spatial variability of the exposure scores is illustrated in Figure 8, highlighting that, apart from the BBs that accommodate some kind of critical infrastructure the highest scores are concentrated close to the city centre.

4.8. Selection and scoring of the hazard indicators for the flash flood peril

For the hazard component of the risk, a probabilistic flash flood hazard assessment is considered for the case study application. The assessment provides the maximum expected flood inundation depth in the area around the Seveso River considering a 10-year mean return period event. The referred data is offered in a resolution that is higher than the one adopted in this study (i.e. several flood inundation depth estimates are available within the boundaries of a BB). In order to translate the referred data into BB hazard scores, the simulated flood inundation depths, that are encountered within the boundaries of each BB, are initially averaged to obtain a mean flood inundation depth per BB. Figure 9(a) [and Figure 9(b) in enlarged view] shows the spatial distribution of the mean flood

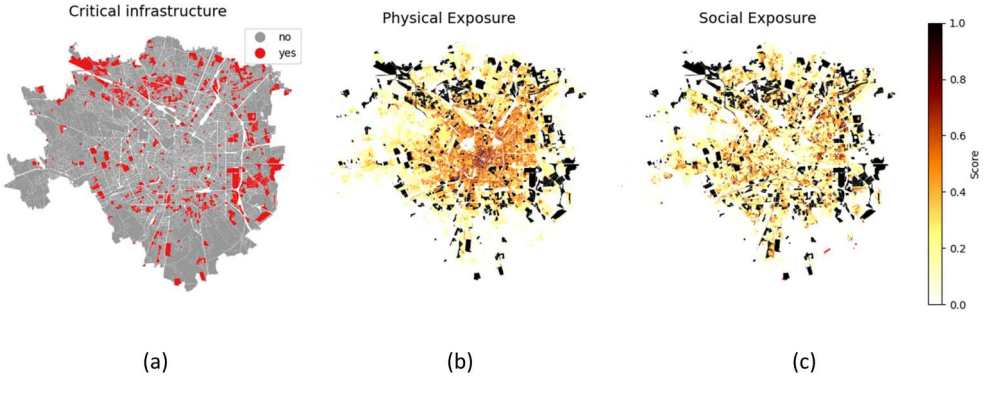

Figure 7. (a) Existence of critical infrastructure in the city of Milan and spatial variability of (b) physical and (c) social exposure scores.

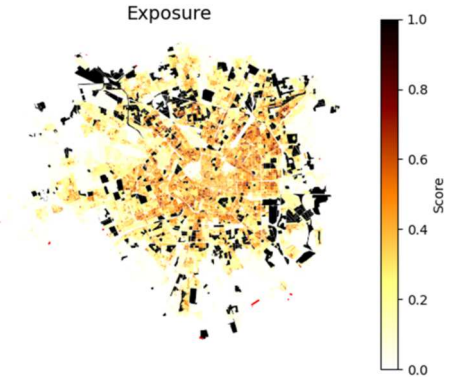

Figure 8. Spatial variability of the exposure score.

inundation depth of the considered flash flood scenario expressed in a BB resolution level. The flood inundation depths (Intensity1, FID) are translated into hazard scores according to Table A of the Supplementary file and Equation (13), using a likelihood score equal to 1, essentially treating the hazard scenario as deterministic (see Section 3.5). This approach was only employed herein to allow comparisons with an actual past flash flood event that occurred in the same region and for which the consequences are known. For this past event, the reported inundation depths compare well with those of the adopted hazard scenario and hence will be used, later on in this study, for validating the proposed framework. The spatial distribution of the flash flood hazard scores in the affected area is illustrated in Figure 9(c).

The past event that will be used for validation purposes, corresponds to the July 8th, 2014 flash flood incident that occurred following a heavy precipitation event and resulted in severe economic losses (~55 M€ according to Ravazzani et al., 2016). The heavy rain overflowed the Seveso River–having its course extending from the Como lake to the city of Milan and running mainly underground in the urban areas (Vitale et al., 2020). The affected areas have been indicated by the Urban Resilience Department of the

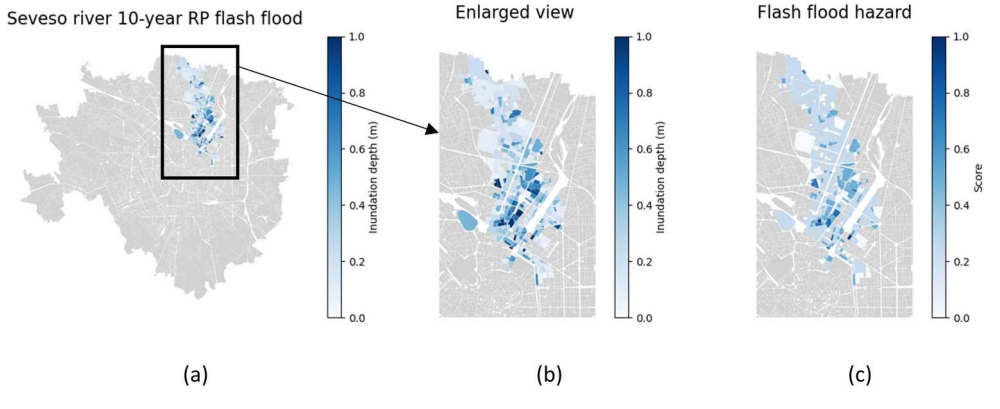

Figure 9. (a) Spatial variability of the mean flood inundation depth due to the Seveso River flash flood scenario with a 10-year mean return period, (b) enlarged view of the hazard scenario, and (c) flash flood hazard score.

Municipality of Milan (personal communication) and are superimposed with the considered probabilistic flash flood scenario in Figure 10 to verify similarities. As such, during the July 8th event, the Seveso River flood affected the Niguarda district (Figure 10-Area 1), near via Ca' Granda (Figure 10-Area 3). In particular, water overflowing from the manholes and creating fountains of water and mud was reported, that completely flooded viale Zara and the entire district (Figure 10-Area 2). The area affected by the flood also involved the Isola district (Figure 10-Area 4), located close to the historic centre of Milan, which resulted in Piazza Minniti and neighbouring streets being completely flooded. It was also reported that in many streets the flood inundation depth reached 50–60 cm.

4.9. Risk score estimates for the case study application

4.9.1. Verification of the proposed framework and baseline assessment

The risk score is calculated according to Equation (14) for each BB as the geometric mean of the three risk components scores, that is, vulnerability, exposure and hazard, and the spatially variable risk scores for all BBs in the affected part of the city are presented in Figure 11 for the baseline assessment ('as is').

Figure 11 shows that the risk scores range from 0 to 0.66, while only a few BBs have risk scores higher than 0.5. It is further observed that the highest risk scores are encountered in BBs within the Isola district (Area 4 in Figure 10). This district, according to the information provided by the Urban Resilience Department of the Municipality of Milan, was heavily affected by the July 8th 2014 event, with extensive damages to cars, shops, basements and ground floors of many homes being reported. For the remaining areas that sustained some sort of damage, the framework yields lower risk scores, while the region in the north of the Niguarda district, that suffered no remarkable damage during the referred past flash flood event, has the lowest risk scores. It can be thus inferred, that the applied framework was able to successfully identify the most stressed parts of the city.

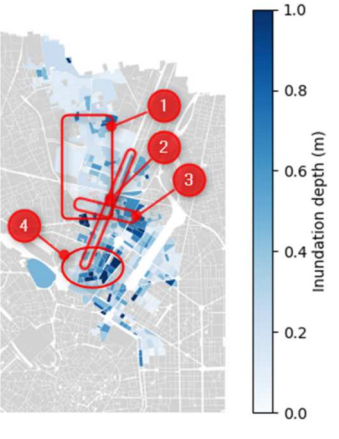

Figure 10. Areas affected by the flash flood event on July 8th, 2014 in the city of Milan: (1) Niguarda district, (2) via Ca' Granda, (3) viale Zara, and (4) Isola district. The mean flood depth due to the Seveso River flash flood scenario with a 10-year mean return period is superimposed for comparison.

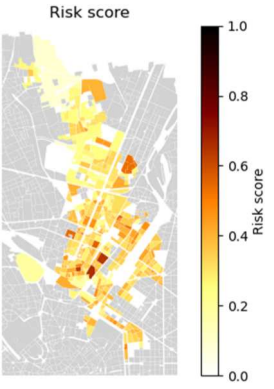

Figure 11. Spatial variability of the risk score – baseline assessment.

The identification of the most stressed parts of the city considering the existing (if any) COPs, corresponds to the so-called 'baseline assessment' and can be further exploited, within the context of a first-level risk-aware DSS, for assisting decision makers to (a) direct their actions in those parts of the city that are needed most and (b) assess the efficiency of alternative mitigation measures in reducing the risk. The implementation of these measures/actions, which have been translated within the context of the proposed framework into COP indicators, is expected to initially have an effect on the vulnerability score and ultimately on the risk score (risk mitigation scenario).

To demonstrate how the proposed framework could be utilised in the context of a DSS for the prioritisation of the risk proactive mitigation actions, two risk mitigation scenarios will be examined. These scenarios will sequentially implement two mitigation measures, one with local and one with global scale effects. The mitigation measures will be implemented in addition to the already existing COPs in order to further reduce the risk score in the most stressed city areas, as those were identified by the baseline assessment. The lowering of the risk score in the investigated BBs is due to the reduction of the vulnerability score as this is evaluated by means of the indicators summarised in Table 2. Through implementing more adaptation measures (on a global or local scale) the vulnerability and hence the risk score in their zones of influence is reduced since the copying capacity dimension increases. Three BBs, i.e. BB1, BB2 and BB3 illustrated in Figure 12 (a), are selected and consequently analysed. The risk component scores and risk scores for the selected BBs are presented in Table 2. According to the baseline assessment (first row of Table 2), BB1 and BB2 have the highest risk scores, equal to 0.66 and 0.64, respectively, and vulnerability scores equal to 0.37 and 0.35, respectively, while BB3

Table 2. Vulnerability and risk assessment of the considered BBs.

	Hazard score			Exposure score			Vulnerability score			Risk score		
	BB1	BB2	BB3	BB1	BB2	BB3	BB1	BB2	BB3	BB1	BB2	BB3
Baseline assessment	0.75	0.75	0.5	1.0	1.0	1.0	0.37	0.35	0.34	0.66	0.64	0.56
Mitigation scenario 1: COP5 in BB1							0.30	0.35	0.34	0.61	0.64	0.56
Mitigation scenario 2: COP5 in BB1 and COP4							0.09	0.14	0.13	0.40	0.47	0.41

Note: Scores before and after the implementation of two additional COPs.

possesses a vulnerability score that is comparable to those that are reported for BB1 and BB2, but it is associated with a lower risk score, i.e. 0.56, due to the lower hazard score in that particular BB. All three BBs have exposure scores that are equal to 1, i.e. the highest possible exposure score (essentially implying the presence of critical infrastructure for the case at hand).

4.9.2. Risk mitigation scenarios

In the first mitigation scenario (Risk mitigation scenario 1), the reduction of the risk score of BB1, which is the highest encountered among the considered BBs, is achieved by implementing a local intervention measure. Local intervention measures primarily affect the performance of the BBs in which they are implemented and possibly that of neighbouring BBs (depending on the size and shape of the BBs), while they do not have any impact on distant BBs. Despite their limited distant effect, local interventions usually require less time and resources compared to global ones and hence their implementation is justified in regions that have only a few BBs with high risk scores and/or the available budget is limited. As such, COP5 is implemented in BB1 and hence the percentage of greenery in the referred BB is increased from 4.5% to 60%. The final/total percentage of greenery (i.e. 60%) is considered for the determination of the score of COP5 of BB1 for the mitigation scenario.

The effect of implementing COP5 in BB1 is reflected in both its vulnerability and risk scores, as shown in the second row of Table 2 (Mitigation scenario 1). In this case, the vulnerability score decreased from 0.37 to 0.30 (~19% reduction), while the risk score was reduced from 0.66 to 0.61 (~8% reduction). At the same time, the vulnerability and risk scores in BB2 and BB3 remained, as expected, unaffected, since they lie outside the 100 m radius that is likely to be affected but this local COP. The risk scores of all BBs for the first risk mitigation scenario are illustrated in Figure 12(b). It is important to note that due to the implementation of this mitigation measure, BB1 does not possess the maximum vulnerability and risk scores among the considered BBs. Instead, BB2 with a vulnerability score equal to 0.35 and a risk score equal to 0.64 (the same scores as in the baseline assessment) now has the highest scores. Furthermore, although the

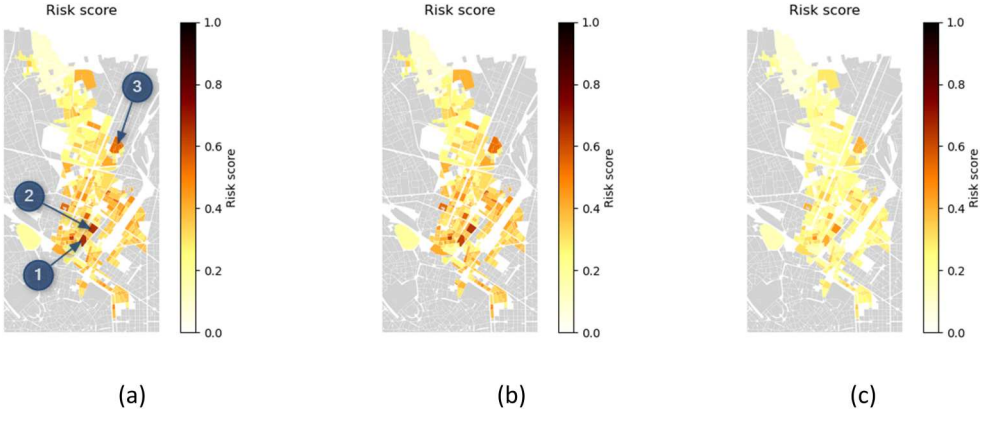

Figure 12. (a) BB identification and risk scores for the baseline assessment, (b) risk scores for risk mitigation scenario 1, and (c) risk scores for risk mitigation scenario 2.

vulnerability score of BB1 due to the implementation of COP5 is lower than that of BB3 (vulnerability score of BB3 is 0.34, the same as in the baseline assessment), its risk score still remains higher than that of BB3 (risk score of BB3 is 0.34, the same as in the baseline assessment) due to the effect of the hazard component of the risk, that for BB1 receives a higher score compared to BB3.

In the second mitigation scenario (Mitigation scenario 2) an additional to the local COP5 mitigation measure is implemented, in an attempt to further mitigate the risk. In particular, the construction of a flood protection infrastructure (COP4) as per the latest design regulations, which is a global scale intervention measure, is implemented in additional to the existing COPs and the local COP5 intervention that was implemented before in BB1. The resulting vulnerability and risk scores following the implementation of this additional measure are presented in the third row of Table 2 (Mitigation scenario 2) for the three examined BBs, while the risk scores of all BBs are also illustrated in Figure 12(c).

Contrary to the rather limited positive impact of COP5, the implementation of COP4 is seen to have a more significant effect on the risk scores of the BBs across the examined region. The latter observation was expected due to the higher efficiency of this COP measure that is reflected in its weight and also due to its global nature. It is thus observed that the vulnerability scores of BB2 and BB3 were reduced by 60% and ~62%, respectively, while the vulnerability score of BB1, which has the cumulative positive effect of both COP4 and COP5, was decreased by ~76% (with respect to the baseline assessment), reaching a value of only 0.09. As far as the risk scores are concerned, risk scores of both BB2 and BB3 dropped by ~27%, with BB2 still exhibiting the highest risk score, that however was reduced to a value that is lower than 0.5. The risk score of BB1, on the other hand, decreased by 34%, reaching a value of 0.40 that is even lower compared to that of BB3 (0.41), highlighting the effectiveness of implementing multiple COPs.

5. Conclusions

The proposed indicator-based vulnerability and risk assessment framework is flexible, adjustable and suitable for being implemented within a first-order risk-aware DSS that aims at enabling the prioritisation of proactive adaptation actions against future hazardous events that are likely to affect an urban network. It is mainly addressed to city authorities and urban planners and its purpose is to identify the most stressed parts of a city in case that those are affected by a particular peril.

The output of the proposed framework is offered in the form of spatially variable vulnerability, exposure, hazard and risk scores evaluated for certain hazard scenarios. In addition to the baseline assessment, that is, the risk assessment that is undertaken to evaluate risk scores for the 'as is' state of the city, the framework offers the possibility to analyse the effectiveness of alternative risk mitigation scenarios in order to assist decision-makers identifying the most appropriate proactive measures. Its formulation is generic and it can be utilised, with appropriate adjustments, for undertaking a vulnerability and risk assessment against a variety of perils in urban-scale applications, while for the purpose of the present study, the framework was demonstrated for the flash flood peril. The scope and applicability of the proposed easy-to-implement framework is restricted to the identification of the most stressed parts of a city, should the latter

be exposed to a particular hazard, and the comparative assessment of the mitigating effect of alternative proactive actions on the risk. More detailed modelling, analysis and assessment should follow in order to account for supplementary, yet equally important aspects, such as the budget, time, regulation and other constraints that are relevant to the actual implementation of the mitigation measures. Furthermore, the proposed framework is sensitive to the adopted weighting scheme for which further research is required to provide more robust evidence. It is also worth mentioning that indicators could be not only peril-specific, but also location-specific and thus appropriate adjustments are likely to be needed to account for the particularities of the considered city network. As a final note, it should be noted that several key sustainability-related aspects (e.g. longevity of the investigated adaptation measures, protection and rational use of natural resources) were only partially considered or disregarded in this study, that is mainly focused on offering a preliminary identification of the most efficient, risk mitigation-wise, adaptation measures across an urban network.

Acknowledgements

The authors would like to thank Christos Kontopoulos, Efthymios Magkoufis and Anna Papadima for providing the exposure data for the city of Milan, Jaakko Ikonen for providing the flash flood hazard, and Silvia Rossi for providing information about a past flash flood event that affected the city of Milan. Special thanks also to Associate Prof. Dimitrios Vamvatsikos and Dr. Konstantinos Bakalis for the fruitful discussions during the development of the presented framework. The authors are grateful to the anonymous reviewers for their valuable suggestions to improve the quality of the paper.

Disclosure statement

No potential conflict of interest was reported by the author(s).

Funding

This research has received funding from the EU Horizon 2020 research and innovation programme HARMONIA, entitled 'Development of a Support System for Improved Resilience and Sustainable Urban areas to cope with Climate Change and Extreme Events based on GEOSS and Advanced Modelling Tools' under agreement No. 101003517.

ORCID

Despoina Skoulidou http://orcid.org/0000-0002-4053-1127
Athanasia K. Kazantzi http://orcid.org/0000-0002-5233-6740

References

Abdrabo, K. I., Kantoush, S. A., Esmaiel, A., Saber, M., Sumi, T., Almamari, M., Elboshy, B., & Ghoniem, S. (2023). An integrated indicator-based approach for constructing an urban flood vulnerability index as an urban decision-making tool using the PCA and AHP techniques: A case study of Alexandria, Egypt. *Urban Climate*, *48*, 101426. https://doi.org/10.1016/j.uclim.2023.101426

Adger, W. N. (2006). Vulnerability. *Global Environmental Change*, *16*(3), 268–281. https://doi.org/10.1016/j.gloenvcha.2006.02.006

Balica, S. F., Wright, N. G., & Van der Meulen, F. (2012). A flood vulnerability index for coastal cities and its use in assessing climate change impacts. *Natural Hazards*, *64*(1), 73–105. https://doi.org/10.1007/s11069-012-0234-1

Becciu, G., Ghia, M., & Mambretti, S. (2018). A century of works on River Seveso: From unregulated development to basin reclamation. *International Journal of Environmental Impacts: Management, Mitigation and Recovery*, *1*(4), 461–472. https://doi.org/10.2495/EI-V1-N4-461-472

Bigi, V., Comino, E., Fontana, M., Pezzoli, A., & Rosso, M. (2021). Flood vulnerability analysis in urban context: A socioeconomic sub-indicators overview. *Climate*, *9*(1), 12. https://doi.org/10.3390/cli9010012

Birkmann, J. (2007). Risk and vulnerability indicators at different scales: Applicability, usefulness and policy implications. *Environmental Hazards*, *7*(1), 20–31. https://doi.org/10.1016/j.envhaz.2007.04.002

Birkmann, J. (2013). *Measuring vulnerability to natural hazards: Towards disaster resilient societies* (2nd ed.). United Nations University Press.

Bruneau, M., Chang, S. E., Eguchi, R. T., Lee, G. C., O'Rourke, T. D., Reinhorn, A. M., Shinozuka, M., Tierney, K., Wallace, W. A., & Von Winterfeldt, D. (2003). A framework to quantitatively assess and enhance the seismic resilience of communities. *Earthquake Spectra*, *19*(4), 733–752. https://doi.org/10.1193/1.1623497

Chang, H., Pallathadka, A., Sauer, J., Grimm, N. B., Zimmerman, R., Cheng, C., Iwaniec, D. M., Kim, Y., Lioyd, R., McPhearson, T., Rosenzweig, B., Troxler, T., Welty, C., Brenner, R., & Herreros-Cantis, P. (2021). Assessment of urban flood vulnerability using the social-ecological-technological systems framework in six US cities. *Sustainable Cities and Society*, *68*, 102786. https://doi.org/10.1016/j.scs.2021.102786

Ciurean, R. L., Schroter, D., & Glade, T. (2013). Conceptual frameworks of vulnerability assessments for natural disasters reduction. In J. Tiefenbacher (Ed.), *Approaches to disaster management—Examining the implications of hazards, emergencies and disasters* (pp. 3–31). London: IntechOpen. https://doi.org/10.5772/55538.

Collins, M., Dasgupta, S., & Schapire, R. E. (2002). A generalization of principal components analysis to the exponential family. In T. Dietterich, S. Becker, & Z. Ghahramani (Eds.), *Advances in Neural Information Processing Systems* (Vol. 14, pp. 617–624). Cambridge, MA: MIT Press.

IPCC. (2014). Climate change 2014: Synthesis report. In Core Writing Team, R. K. Pachauri, & L. A. Meyer (Eds.), *Contribution of Working Groups I, II and III to the Fifth Assessment Report of the Intergovernmental Panel on Climate Change* (pp. 151).

IPCC. (2023). Sections. In Core Writing Team, H. Lee, & J. Romero (Eds.), *Climate Change 2023: Synthesis report. Contribution of Working Groups I, II and III to the Sixth Assessment Report of the Intergovernmental Panel on Climate Change* (pp. 35–115). IPCC. https://doi.org/10.59327/IPCC/AR6-9789291691647.

Cutter, S. L., Boruff, B. J., & Shirley, W. L. (2003). Social vulnerability to environmental hazards. *Social Science Quarterly*, *84*(2), 242–261. https://doi.org/10.1111/1540-6237.8402002

Cutter, S. L., Burton, C. G., & Emrich, C. T. (2010). Disaster resilience indicators for benchmarking baseline conditions. *Journal of Homeland Security and Emergency Management*, *7*(1), https://doi.org/10.2202/1547-7355.1732

Cutter, S. L., & Derakhshan, S. (2020). Temporal and spatial change in disaster resilience in US counties, 2010–2015. *Environmental Hazards*, *19*(1), 10–29. https://doi.org/10.1080/17477891.2018.1511405

Esty, D. C., Levy, M., Srebotnjak, T., & de Sherbinin, A. (2005). *Environmental Sustainability Index: Benchmarking national environmental stewardship*. Yale Center for Environmental Law & Policy.

Fekete, A., Damm, M., & Birkmann, J. (2010). Scales as a challenge for vulnerability assessment. *Natural Hazards*, *55*(3), 729–747. https://doi.org/10.1007/s11069-009-9445-5

FEMA. (2019). *National threat and hazard identification and risk assessment (THIRA) overview and methodology*. U.S department of homeland security. https://www.fema.gov/sites/default/files/2020-06/fema_national-thira-overview-methodology_2019_0.pdf

Fuchs, S., Birkmann, J., & Glade, T. (2012). Vulnerability assessment in natural hazard and risk analysis: Current approaches and future challenges. *Natural Hazards*, *64*, 1969–1975. https://doi.org/10.1007/s11069-012-0352-9

Fuchs, S., Karagiorgos, K., Keiler, M., Papathoma-Köhle, M., & Nyberg, L. (2024). The ambiguity in IPCC's risk diagram raises explanatory challenges. *Natural Hazards*. https://doi.org/10.1007/s11069-024-06643-9

Gentile, R., Cremen, G., Galasso, C., Jenkins, L. T., Manandhar, V., Menteşe, E. Y., Guragain, R., & McCloskey, J. (2022). Scoring, selecting, and developing physical impact models for multi-hazard risk assessment. *International Journal of Disaster Risk Reduction*, *82*, 103365. https://doi.org/10.1016/j.ijdrr.2022.103365

Greco, S., Ishizaka, A., Tasiou, M., & Torrisi, G. (2019). On the methodological framework of composite indices: A review of the issues of weighting, aggregation, and robustness. *Social Indicators Research*, *141*(1), 61–94. https://doi.org/10.1007/s11205-017-1832-9

Hawchar, L., Naughton, O., Nolan, P., Stewart, M. G., & Ryan, P. C. (2020). A GIS-based framework for high-level climate change risk assessment of critical infrastructure. *Climate Risk Management*, *29*, 100235. https://doi.org/10.1016/j.crm.2020.100235

Hidayah, E., Wiyono, R. U. A., & Wicaksono, A. D. (2021). Development of the flood vulnerability index using a multi-element approach. *Journal of Water and Land Development*, *50*, 255–264.

International Organisation for Standardization, ISO. (2021). Adaptation to climate change — Guidelines on vulnerability, impacts and risk assessment (ISO 14091:2021).

IPCC. (2019). Technical summary. In H.-O. Pörtner, D. C. Roberts, V. Masson-Delmotte, P. Zhai, M. Tignor, E. Poloczanska, K. Mintenbeck, A. Alegría, M. Nicolai, A. Okem, J. Petzold, B. Rama, & N. M. Weyer (Eds.), *IPCC special report on the ocean and cryosphere in a changing climate* (pp. 39–70). Cambridge University Press. https://doi.org/10.1017/9781009157964.002.

IPCC. (2022a). Climate change 2022: Impacts, adaptation and vulnerability. In H.-O. Pörtner, D. C. Roberts, M. Tignor, E. S. Poloczanska, K. Mintenbeck, A. Alegría, M. Craig, S. Langsdorf, S. Löschke, V. Möller, A. Okem, & B. Rama (Eds.), *Contribution of Working Group II to the Sixth Assessment Report of the Intergovernmental Panel on Climate Change* (pp. 3056). Cambridge University Press. https://doi.org/10.1017/9781009325844.

IPCC. (2022b). Annex I: Glossary [van Diemen, R., J.B.R. Matthews, V. Möller, J.S. Fuglestvedt, V. Masson-Delmotte, C. Méndez, A. Reisinger, S. Semenov (eds)]. IPCC, 2022: Climate Change 2022: Mitigation of Climate Change. Contribution of Working Group III to the Sixth Assessment Report of the Intergovernmental Panel on Climate Change [P.R. Shukla, J. Skea, R. Slade, A. Al Khourdajie, R. van Diemen, D. McCollum, M. Pathak, S. Some, P. Vyas, R. Fradera, M.

Kang, H.-s., & Kim, Y.-t. (2016). The physical vulnerability of different types of building structure to debris flow events. *Natural Hazards*, *80*(3), 1475–1493. https://doi.org/10.1007/s11069-015-2032-z

Kappes, M. S., Papathoma-Köhle, M., & Keiler, M. (2012). Assessing physical vulnerability for multi-hazards using an indicator-based methodology. *Applied Geography*, *32*(2), 577–590. https://doi.org/10.1016/j.apgeog.2011.07.002

Karagiorgos, K., Thaler, T., Hübl, J., Maris, F., & Fuchs, S. (2016). Multi-vulnerability analysis for flash flood risk management. *Natural Hazards*, *82*(S1), 63–87. https://doi.org/10.1007/s11069-016-2296-y

Kelman, I. (2018). Lost for words amongst disaster risk science vocabulary? *International Journal of Disaster Risk Science*, *9*(3), 281–291. https://doi.org/10.1007/s13753-018-0188-3

Kim, H., Lee, D. K., & Sung, S. (2016). Effect of urban green spaces and flooded area type on flooding probability. *Sustainability*, *8*(2), 134. https://doi.org/10.3390/su8020134

Kontopoulos, C., Magkoufis, E., Papadima, A., Skoulidou, D., Kazantzi, A., & Hafner, S.. (2023). A novel web-based decision support tool for enhancing urban resilience and sustainability. In *Ninth International Conference on Remote Sensing and Geoinformation of the Environment (RSCy2023)* (Vol. 12786, pp. 326–337). SPIE.

Krellenberg, K., & Welz, J. (2017). Assessing urban vulnerability in the context of flood and heat hazard: Pathways and challenges for indicator-based analysis. *Social Indicators Research*, *132*(2), 709–731. https://doi.org/10.1007/s11205-016-1324-3

Kumar, M., Kalra, N., Singh, H., Sharma, S., Rawat, P. S., Singh, R. K., Gupta, A. K., Kumar, P., & Ravindranath, N. H. (2021). Indicator-based vulnerability assessment of forest ecosystem in the Indian Western Himalayas: An analytical hierarchy process integrated approach. *Ecological Indicators*, *125*, 107568. https://doi.org/10.1016/j.ecolind.2021.107568

Leal, M., Reis, E., Pereira, S., & Santos, P. P. (2021). Physical vulnerability assessment to flash floods using an indicator-based methodology based on building properties and flow parameters. *Journal of Flood Risk Management*, *14*(3), e12712. https://doi.org/10.1111/jfr3.12712

Liverman, D. M. (1990). Chapter 26. Vulnerability to global environmental change. In R. E. Kasperson (Ed.), *Understanding global environmental change: The contributions of risk analysis and management* (pp. 27–44). Clark University.

Loli, M., Mitoulis, S. A., Kefalas, G., Bouzoni, E., Kapetas, L., Diaz-Fanas, G., & Arroyo, F. A. (2022). *Flood risk for urban mobility in Maputo, Mozambique: Regional-scale indexing based on earth observation and demographic data*. 3rd International Conference on Natural Hazards & Infrastructure, 5-7 July 2022, Athens, Greece.

Maranzoni, A., D'Oria, M., & Rizzo, C. (2023). Quantitative flood hazard assessment methods: A review. *Journal of Flood Risk Management*, *16*(1), e12855. https://doi.org/10.1111/jfr3.12855

Marin-Ferrer, M., Vernaccini, L., & Poljansek, K. (2017). Index for Risk Management INFORM Concept and Methodology Report — Version 2017, EUR 28655 EN. https://doi.org/10.2760/094023.

Mikulic, J., Kozic, I., & Kresic, D. (2015). Weighting indicators of tourism sustainability: A critical note. *Ecological Indicators*, *48*, 312–314. https://doi.org/10.1016/j.ecolind.2014.08.026

Mitoulis, S. A., Bompa, D. V., & Argyroudis, S. (2023). Sustainability and climate resilience metrics and trade-offs in transport infrastructure asset recovery. *Transportation Research Part D: Transport and Environment*, *121*, 103800. https://doi.org/10.1016/j.trd.2023.103800

Moreira, L. L., de Brito, M. M., & Kobiyama, M. (2021). Review article: A systematic review and future prospects of flood vulnerability indices. *Natural Hazards and Earth System Sciences*, *21*(5), 1513–1530. https://doi.org/10.5194/nhess-21-1513-2021

Morrison, D., Beevers, L., Wright, G., & Stewart, M. D. (2022). The impact of data spatial resolution on flood vulnerability assessment. *Environmental Hazards*, *21*(1), 77–98. https://doi.org/10.1080/17477891.2021.1912694

Muller, A., Reiter, J., & Weiland, U. (2011). Assessment of urban vulnerability towards floods using an indicator-based approach – A case study for Santiago de Chile. *Natural Hazards and Earth System Sciences*, *11*(8), 2107–2123. https://doi.org/10.5194/nhess-11-2107-2011

Murphy, L. B., & Moriarty, A. E. (1976). *Vulnerability, coping and growth from infancy to adolescence*. Oxford: Yale University Press.

Nelson, L., & Ahmadpoor, N. (2023). An examination of flood resilience in London Borough of Southwark. *Urban Climate*, *52*, 101692. https://doi.org/10.1016/j.uclim.2023.101692

Nguyen, T. T., Bonetti, J., Rogers, K., & Woodroffe, C. D. (2016). Indicator-based assessment of climate-change impacts on coasts: A review of concepts, methodological approaches and vulnerability indices. *Ocean & Coastal Management*, *123*, 18–43. https://doi.org/10.1016/j.ocecoaman.2015.11.022

Niehoff, D., Fritsch, U., & Bronstert, A. (2002). Land-use impacts on storm-runoff generation: Scenarios of land-use change and simulation of hydrological response in a meso-scale catchment in SW-Germany. *Journal of Hydrology*, *267*(1-2), 80–93. https://doi.org/10.1016/S0022-1694(02)00142-7

Papathoma-Köhle, M. (2016). Vulnerability curves vs. vulnerability indicators: Application of an indicator-based methodology for debris-flow hazards. *Natural Hazards and Earth System Sciences*, *16*(8), 1771–1790. https://doi.org/10.5194/nhess-16-1771-2016

Papathoma-Köhle, M., Cristofari, G., Wenk, M., & Fuchs, S. (2019). The importance of indicator weights for vulnerability indices and implications for decision making in disaster management. *International Journal of Disaster Risk Reduction*, *36*, 101103. https://doi.org/10.1016/j.ijdrr.2019.101103

Papathoma-Köhle, M., Gems, B., Sturm, M., & Fuchs, S. (2017). Matrices, curves and indicators: A review of approaches to assess physical vulnerability to debris flows. *Earth-Science Reviews*, *171*, 272–288. https://doi.org/10.1016/j.earscirev.2017.06.007

Pathak, S., Panta, H. K., Bhandari, T., & Paudel, K. P. (2020). Flood vulnerability and its influencing factors. *Natural Hazards*, *104*(3), 2175–2196. https://doi.org/10.1007/s11069-020-04267-3

Rana, I. A., & Routray, J. K. (2018a). Integrated methodology for flood risk assessment and application in urban communities of Pakistan. *Natural Hazards*, *91*(1), 239–266. https://doi.org/10.1007/s11069-017-3124-8

Rana, I. A., & Routray, J. K. (2018b). Multidimensional model for vulnerability assessment of urban flooding: An empirical study in Pakistan. *International Journal of Disaster Risk Science*, *9*(3), 359–375. https://doi.org/10.1007/s13753-018-0179-4

Ravazzani, G., Amengual, A., Ceppi, A., Homar, V., Romero, R., Lombardi, G., & Mancini, M. (2016). Potentialities of ensemble strategies for flood forecasting over the Milano urban area. *Journal of Hydrology*, *539*, 237–253. https://doi.org/10.1016/j.jhydrol.2016.05.023

Saaty, T. L. (1990). How to make a decision: The analytic hierarchy process. *European Journal of Operational Research*, *48*(1), 9–26. https://doi.org/10.1016/0377-2217(90)90057-I

Saisana, M., & Tarantola, S. (2002). *State-of-the-art report on current methodologies and practices for composite indicator development* (Vol. 214, pp. 4–15). Ispra, Italy: European Commission, Joint Research Centre, Institute for the Protection and the Security of the Citizen, Technological and Economic Risk Management Unit.

Schmidtlein, M. C., Deutsch, R. C., Piegorsch, W. W., & Cutter, S. L. (2008). A sensitivity analysis of the social vulnerability index. *Risk Analysis*, *28*(4), 1099–1114. https://doi.org/10.1111/j.1539-6924.2008.01072.x

Silva, M., & Pereira, S. (2014). Assessment of physical vulnerability and potential losses of buildings due to shallow slides. *Natural Hazards*, *72*(2), 1029–1050. https://doi.org/10.1007/s11069-014-1052-4

Simmons, D. C., Corbane, C., Menoni, S., Schneiderbauer, S., & Zschau, J. (2017). Understanding disaster risk: Risk assessment methodologies and examples. In K. Poljanšek, M. Marín Ferrer, T. De Groeve, & I. Clark (Eds.), *Science for disaster risk management 2017: Knowing better and losing less* (pp. 38–130). EUR 28034 EN, Publications Office of the European Union.

Stephens, K. K., Blessing, R., Tasuji, T., McGlone, M. S., Stearns, L. N., Lee, Y., & Brody, S. D. (2024). Investigating ways to better communicate flood risk: The tight coupling of perceived flood map usability and accuracy. *Environmental Hazards*, *23*(1), 92–111. https://doi.org/10.1080/17477891.2023.2224956

Stephenson, V., & D'Ayala, D. (2014). A new approach to flood vulnerability assessment for historic buildings in England. *Natural Hazards and Earth System Sciences*, *14*(5), 1035–1048. https://doi.org/10.5194/nhess-14-1035-2014

Sun, L., & Liu, X. (2024). Identifying different frames of resilience–vulnerability nexus in disaster study. *Environmental Hazards*, *23*(2), 113–129. https://doi.org/10.1080/17477891.2023.2220948

Taramelli, A., Righini, M., Valentini, E., Alfieri, L., Gatti, I., & Gabellani, S. (2022). Building-scale flood loss estimation through vulnerability pattern characterization: Application to an urban flood in Milan, Italy. *Natural Hazards and Earth System Sciences*, *22*(11), 3543–3569. https://doi.org/10.5194/nhess-22-3543-2022

Thouret, J. C., Ettinger, S., Guitton, M., Santoni, O., Magill, C., Martelli, K., Zuccaro, G., Revilla, V., Charca, J. A., & Arguedas, A. (2014). Assessing physical vulnerability in large cities exposed to flash floods and debris flows: The case of Arequipa (Peru). *Natural Hazards*, *73*(3), 1771–1815. https://doi.org/10.1007/s11069-014-1172-x

United Nations International Strategy for Disaster Reduction (UNISDR). (2015). *Sendai framework for disaster risk reduction 2015–2030*.

United Nations Office for Disaster Risk Reduction (UNDRR). (2016). *Report of the open ended intergovernmental expert working group on indicators and terminology relating to disaster risk reduction*. (A/71/644).

Vitale, C., & Meijerink, S. (2021). Understanding inter-municipal conflict and cooperation on flood risk policies for the metropolitan city of Milan. *Water Alternatives*, *14*(2), 597–618.

Vitale, C., Meijerink, S., Moccia, F. D., & Ache, P. (2020). Urban flood resilience, a discursive-institutional analysis of planning practices in the metropolitan city of Milan. *Land Use Policy*, *95*, 104575. https://doi.org/10.1016/j.landusepol.2020.104575

Waseem, H. B., & Rana, I. A. (2023). Floods in Pakistan: A state-of-the-art review. *Natural Hazards Research*, *3*, 359–373. https://doi.org/10.1016/j.nhres.2023.06.005

Wisner, B., Blaikie, P., Cannon, T., & Davis, I. (2004). *At risk: Natural hazards, people's vulnerability and disasters*. Routledge.

Wolf, S. (2012). Vulnerability and risk: Comparing assessment approaches. *Natural Hazards*, *61*(3), 1099–1113. https://doi.org/10.1007/s11069-011-9968-4

Yuan, Y. (2008). Impact of intensity and loss assessment following the great Wenchuan Earthquake. *Earthquake Engineering and Engineering Vibration*, *7*(3), 247–254. https://doi.org/10.1007/s11803-008-0893-9

Zhen, Y., Liu, S., Zhong, G., Zhou, Z., Liang, J., Zheng, W., & Fang, Q. (2022). Risk assessment of flash flood to buildings using an indicator-based methodology: A case study of mountainous rural settlements in southwest China. *Frontiers in Environmental Science*, *10*, 931029. https://doi.org/10.3389/fenvs.2022.931029

Zischg, A. P., Röthlisberger, V., Mosimann, M., Profico-Kaltenrieder, R., Bresch David, N., Fuchs, S., Kauzlaric, M., & Keiler, M. (2021). Evaluating targeted heuristics for vulnerability assessment in flood impact model chains. *Journal of Flood Risk Management*, *14*(4), e12736. https://doi.org/10.1111/jfr3.12736